Global and Compact Meshless Schemes for the Unsteady Convection-Diffusion Equation

K. Djidjeli [1], P. P. Chinchapatnam [1], P. B. Nair [1], W.G. Price [2]

[1] School of Engineering Sciences, Computational Engineering and Design Group, University of Southampton, Southampton SO17 1BJ, U.K.
[2] School of Engineering Sciences, Ship Science, University of Southampton, Southampton, SO17 1BJ, UK

Abstract

The numerical solution of convection-diffusion equation has been a long standing problem and many numerical schemes which attempt to find stable and accurate solutions for convection dominated cases have to resort to artificial dissipation to stabilize the numerical solution. In this paper, we investigate the application of global and compact meshless collocation techniques with radial basis functions for solving the unsteady convection-diffusion equation. We employ the method of lines approach to discretize the governing operator equation. The stability of both explicit and implicit time stepping schemes are analyzed. Numerical results are presented for one-dimensional and two-dimensional problems using various globally supported radial basis functions such as multiquadric (MQ), inverse multiquadric (IMQ), Gaussian, thin plate splines (TPS) and quintics. Numerical studies suggest the global MQ, IMQ and Guassian (when the shape parameter is proprely tuned) have very high convergence rate than TPS and quintics, and as the mesh density increases, all the RBFs tend to have the same accuracy. Further it appears that the global meshless collocation techniques require a very dense set of collocation points in order to achieve accurate results for high Péclet numbers. For the compact supported RBFs, it is found that as the support parameter is increased, the sparsity decreases resulting in a better accuracy but at additional computational cost.

keywords: convection-diffusion; radial basis functions (RBF); collocation;

1 Introduction

The convection diffusion equation is widely used to model a variety of biological (heat transfer in living tissue [1], population dynamics [2]), physical, chemical, economical and financial forecasting processes to name a few [3]. The peculiarity of this equation is that it represents the coupling of two different phenomena, convection and diffusion. It also serves as a simplified model problem to the Navier-Stokes equation in fluid dynamics. The complete numerical solution of this problem has evaded researchers until now. One major difficulty arises from the fact that when the convective term dominates, the approximation can be contaminated due to spurious oscillation and numerical diffusion [4]. The governing equation is parabolic for diffusion dominated cases and turns hyperbolic for convection dominated cases. Traditionally, Finite Difference (FD) and Finite Element (FE) schemes have been utilized to solve the convection-diffusion equation. These schemes work well for diffusion dominated problems. However, when the convective term dominates, special methods with artificial viscosity, upwinding etc., have to be used to stabilize the numerical scheme [5]. All the above schemes are grid based schemes which need a discretization of the domain into elements, which in itself can be a non-trivial task for complicated domains.

In 1990, Kansa [6, 7] introduced a novel approach for solving partial differential equations (PDEs) by collocation motivated by advances in function approximation using radial basis functions (RBFs). In this approach, the solution is approximated using RBFs as trial functions and the collocation technique is used to compute the undetermined coefficients. This is a truly meshless scheme since it only makes use of a scattered set of collocation points and no connectivity information is required. Table 1 lists some of the most commonly used RBFs in the literature [8]. As usual, $r = \| \cdot \|$ denotes the Euclidean norm and σ is a shape parameter.

Table 1: Globally supported radial basis functions

$\phi(r) = (1 + \frac{r^2}{\sigma})^{\frac{1}{2}}$	Multiquadrics
$\phi(r) = (r^2 + \sigma^2)^{\frac{-1}{2}}$	Inverse multiquadrics
$\phi(r) = r^4 \log r$	Thin plate splines
$\phi(r) = e^{-\frac{r^2}{\sigma}}$	Gaussians
$\phi(r) = r^3$	Quintic cubic splines

Hardy's multiquadrics (MQ and IMQ), Duchon's Thin Plate Splines (TPS) and Gaussians are the globally supported RBFs which are commonly used in the literature for solving PDEs [9]. MQ, IMQ and Gaussian RBFs include a shape parameter, whose numerical value can be varied to control the domain of influence of the basis function. For example, in the case of the Gaussian RBF, increasing the value of σ leads to flatter basis functions. Another class of RBFs were introduced by Wendland [10], Wu [11], and Buhmann [12]. These functions are compactly supported, i.e., the domain of influence of the RBF extends over a finite region of the domain as opposed to global RBFs whose influence extends over the entire domain. The extent of influence of the compactly supported RBF is controlled by introducing a support parameter.

Globally supported RBFs produce a dense collocation matrix $\mathbf{A}$, which tends to become highly ill-conditioned at the optimal values of the shape parameter [9]. The compactly supported kernels contain a support size parameter by which we can adjust the sparsity of the matrix, thus making $\mathbf{A}$ well-conditioned [13]. However, this advantage comes at the cost of accuracy.

In the present paper, numerical results are presented for the 1D and 2D unsteady convection-diffusion equation. Previous work focusing on the solution of the steady and unsteady convection-diffusion equations using RBFs can be found in the literature, see, for instance, [7, 14, 15] and the references therein. In Section 2, we introduce the method of lines approach for solving the general unsteady convection-diffusion equation using various globally/ compactly supported RBFs meshless collocation techniques. Section 3 presents an analysis of the stability of explicit and implicit time-stepping schemes. Section 4 presents the numerical results for the 1D and 2D problems.

2 Global and Compact Meshless Collocation Schemes

The governing equation of the unsteady convective-diffusion (CD) problem is given by

$$\begin{array}{ll} \frac{\partial u(\boldsymbol{x},t)}{\partial t} + \mathcal{L}u(\boldsymbol{x},t) = f(\boldsymbol{x},t) & \forall \boldsymbol{x} \in \Omega \subset \mathbb{R}^d, t > 0, \\ \mathcal{B}u(\boldsymbol{x},t) = g(\boldsymbol{x},t) & \forall \boldsymbol{x} \in \partial\Omega \subset \mathbb{R}^d, t > 0, \end{array} \tag{1}$$

where $\mathcal{L} = \kappa\nabla^2 + \vec{v}\cdot\nabla$, κ is the diffusion coefficient, $\vec{v}$ is a velocity vector, $u(\boldsymbol{x},t)$ represents a potential function, and $\mathcal{B}$ is a boundary operator, which can be a Dirichlet, Neumann or a mixed operator. Equation (1) has to be supplemented with an initial condition of the form $u(\boldsymbol{x},t) = u_0(\boldsymbol{x})$.

Let the solution $u(\boldsymbol{x},t)$ be approximated by a linear combination of RBFs as

$$u(\boldsymbol{x},t) = \sum_{j=1}^{N} \lambda_j(t)\ \phi(\|\boldsymbol{x}-\boldsymbol{c}_j\|), \tag{2}$$

where $\phi(\|\boldsymbol{x}-\boldsymbol{c}_j\|)\colon \mathbb{R}^d \rightarrow \mathbb{R}$ is a global/compact RBF with center $\boldsymbol{x}_j \in \mathbb{R}^d$. $\lambda_j(t)$, $j=1,2,\ldots,N$ are undetermined RBF coefficients which evolve with time. The centers of the RBFs used in equation (2) are chosen from a cloud of points situated within the domain Ω and on the boundary $\partial\Omega$, i.e., $\mathcal{C} = \{(\boldsymbol{c}_i)|_{i=1,n_d} \in \Omega, (\boldsymbol{c}_i)|_{i=n_d+1,n_d+n_b} \in \partial\Omega\}$, where n_d and n_b denote the number of centers inside the domain and on the boundary, respectively. Henceforth, we shall denote the total number of centers as N ($N = n_d + n_b$). For simplicity of presentation, we consider the case when the set $\mathcal{C}$ coincides with the set of collocation points. Substituting equation (2) in the governing equation (1), leads to

$$\sum_{j=1}^{N} \frac{d\lambda_j}{dt}\phi(\|\boldsymbol{x}_i-\boldsymbol{c}_j\|) = f_i(t) - \sum_{j=1}^{N} \lambda_j \mathcal{L}^x\phi(\|\boldsymbol{x}_i-\boldsymbol{c}_j\|) \qquad i=1,\ldots,n_d, \tag{3}$$

$$\sum_{j=1}^{N} \mathcal{B}^x\phi(\|\boldsymbol{x}_i-\boldsymbol{c}_j\|) = g_i(t) \qquad i=n_d+1,\ldots,n_d+n_b, \tag{4}$$

where $\mathcal{L}^x\phi(\|\boldsymbol{x}_i-\boldsymbol{c}_j\|)$ and $\mathcal{B}^x\phi(\|\boldsymbol{x}_i-\boldsymbol{c}_j\|)$ denote the application of the convection-diffusion and boundary operators on the RBF $\phi(\|\boldsymbol{x}-\boldsymbol{c}\|)$ as a function of the first argument and evaluated at $\boldsymbol{x}_i$.

Equations (3) and (4) can be rewritten in matrix form as

$$\boldsymbol{\Phi}_\mathbf{d}\frac{d\boldsymbol{\lambda}}{dt} = \boldsymbol{f} - \mathcal{L}^x\boldsymbol{\Phi}_\mathbf{d}\boldsymbol{\lambda}, \tag{5}$$

$$\mathcal{B}^x\boldsymbol{\Phi}_\mathbf{b}\boldsymbol{\lambda} = \boldsymbol{g}, \tag{6}$$

where $\boldsymbol{\Phi}_\mathbf{d}$, $\mathcal{L}^x\boldsymbol{\Phi}_\mathbf{d} \in \mathbb{R}^{n_d\times N}$, $\boldsymbol{\lambda} \in \mathbb{R}^N$, $\boldsymbol{f} \in \mathbb{R}^{n_d}$, $\mathcal{B}^x\boldsymbol{\Phi}_\mathbf{b} \in \mathbb{R}^{n_b\times N}$, and $\boldsymbol{g} \in \mathbb{R}^{n_b}$. For sake of clarity, the matrix $\boldsymbol{\Phi}_\mathbf{d}$ can be written in expanded form as

$$\boldsymbol{\Phi}_\mathbf{d} = \begin{bmatrix} \phi(\|\boldsymbol{x}_1-\boldsymbol{c}_1\|) & \cdots & \phi(\|\boldsymbol{x}_1-\boldsymbol{c}_{n_d}\|) & \cdots & \phi(\|\boldsymbol{x}_1-\boldsymbol{c}_N\|) \\ \vdots & \ddots & \vdots & \ddots & \vdots \\ \phi(\|\boldsymbol{x}_{n_d}-\boldsymbol{c}_1\|) & \cdots & \phi(\|\boldsymbol{x}_{n_d}-\boldsymbol{c}_{n_d}\|) & \cdots & \phi(\|\boldsymbol{x}_{n_d}-\boldsymbol{c}_N\|) \end{bmatrix} \in \mathbb{R}^{n_d\times N},$$

and the vectors $\boldsymbol{f} = [f_1\ f_2\cdots f_{n_d}]^\mathrm{T}$, $\boldsymbol{\lambda} = [\lambda_1\ \lambda_2\cdots\lambda_{n_d}\cdots\lambda_N]^\mathrm{T}$ and $\boldsymbol{g} = [g_1\ g_2\cdots g_{n_b}]^\mathrm{T}$.

Using the notation $\boldsymbol{\lambda}^{n+1} = \boldsymbol{\lambda}(t^{n+1})$, where $t^{n+1} = t^n + dt$ and introducing $\theta-$weighting ($0 \leq \theta \leq 1$) in (5)-(6), we get

$$\boldsymbol{\Phi}_\mathbf{d}\{\frac{\boldsymbol{\lambda}^{n+1}-\boldsymbol{\lambda}^n}{dt}\} = \boldsymbol{f}^{n+1} - \{\theta\ \mathcal{L}^x\boldsymbol{\Phi}_\mathbf{d}\boldsymbol{\lambda}^{n+1} + (1-\theta)\ \mathcal{L}^x\boldsymbol{\Phi}_\mathbf{d}\boldsymbol{\lambda}^{\boldsymbol{n}}\}, \tag{7}$$

$$\mathcal{B}^x\boldsymbol{\Phi}_\mathbf{b}\boldsymbol{\lambda}^{n+1} = \boldsymbol{g}^{n+1}. \tag{8}$$

Equations (7) and (8) can be written in compact form as

$$\boldsymbol{\lambda}^{n+1} = \mathbf{H}_+^{-1}\mathbf{H}_-\boldsymbol{\lambda}^n + \mathbf{H}_+^{-1}\boldsymbol{F}^{n+1}, \tag{9}$$

where

$$\mathbf{H}_+ = \begin{bmatrix} \boldsymbol{\Phi}_\mathbf{d} + \theta\ dt\ \mathcal{L}^x\boldsymbol{\Phi}_\mathbf{d} \\ \mathcal{B}^x\boldsymbol{\Phi}_\mathbf{b} \end{bmatrix},\ \mathbf{H}_- = \begin{bmatrix} \boldsymbol{\Phi}_\mathbf{d} - (1-\theta)\ dt\ \mathcal{L}^x\boldsymbol{\Phi}_\mathbf{d} \\ \mathbf{0} \end{bmatrix},\ \boldsymbol{F}^{n+1} = \begin{bmatrix} dt\ \boldsymbol{f}^{n+1} \\ \boldsymbol{g}^{n+1} \end{bmatrix}.$$

Rewriting equation (2) in matrix form as

$$\boldsymbol{u} = \mathbf{A}\boldsymbol{\lambda}, \quad , \quad where \quad \mathbf{A} = \begin{bmatrix} \mathbf{\Phi_d} \\ \mathbf{\Phi_b} \end{bmatrix} \in \mathbb{R}^{N \times N}. \tag{10}$$

Using equation (10), equation (9) can be written as

$$\boldsymbol{u}^{n+1} = \mathbf{A}\mathbf{H}_+^{-1}\mathbf{H}_-\mathbf{A}^{-1}\boldsymbol{u}^n + \mathbf{A}\mathbf{H}_+^{-1}\boldsymbol{F}^{n+1}. \tag{11}$$

Since no theoretical proof exists for the invertibility of the matrix $\mathbf{H}_+$ when $\theta > 0$ [16], it is not possible to show that the collocation scheme is well posed for such cases. For the case of the explicit scheme with $\theta = 0$, only the Gram matrix $\mathbf{A}$ needs to be inverted. Provided the set of collocation points are distinct, the invertibility of this matrix can be guaranteed due to the result of Micchelli [17]. Additionally, for conditionally positive definite RBFs, a polynomial term needs to be appended in equation (2) to guarantee invertibility.

3 Stability Analysis

In this section, an analysis of the stability of the meshless schemes using the matrix method is presented. Let $\boldsymbol{e}^n = \boldsymbol{u}^n - \widetilde{\boldsymbol{u}}^n$, where $\boldsymbol{u}^n$ is the exact solution and $\widetilde{\boldsymbol{u}}^n$ is the numerically computed solution. The equation for the error $\boldsymbol{e}^{n+1}$ in equation (11) can then be written as

$$\boldsymbol{e}^{n+1} = \mathbf{K}\boldsymbol{e}^n, \tag{12}$$

where the amplification matrix $\mathbf{K} = \mathbf{A}\mathbf{H}_+^{-1}\mathbf{H}_-\mathbf{A}^{-1}$. The numerical scheme will be stable if as $n \to \infty$, the error $\boldsymbol{e}^n \to 0$. This can be guaranteed provided $\rho(\mathbf{K}) < 1.0$, where $\rho(\mathbf{K})$ denotes the spectral radius of the amplification matrix. Substituting $\mathbf{K}$ in equation (12), leads to

$$\mathbf{H}_+\mathbf{A}^{-1}\boldsymbol{e}^{n+1} = \mathbf{H}_-\mathbf{A}^{-1}\boldsymbol{e}^n. \tag{13}$$

Assuming Dirichlet boundary conditions (i.e.,$\mathcal{B} = \mathcal{I}$, where $\mathcal{I}$ is the identity operator), equation (13) can be written as

$$[\mathbf{I} + \theta\ dt\ \mathbf{M}]\boldsymbol{e}^{n+1} = [\mathbf{I} - (1-\theta)\ dt\ \mathbf{M}]\boldsymbol{e}^n, \tag{14}$$

where $\mathbf{I} \in \mathbb{R}^{n_d \times N}$ is the identity matrix and the matrix $\mathbf{M} = \mathcal{L}\mathbf{\Phi_d}\mathbf{A}^{-1}$.

It can be seen from equation (14) that stability is assured if all the eigenvalues of the matrix $[\mathbf{I} + \theta\ \delta t\ \mathbf{M}]^{-1}\ [\mathbf{I} - (1-\theta)\ \delta t\ \mathbf{M}]$ are less than unity, i.e.,

$$\left| \frac{1 - (1-\theta)\ dt\ \lambda_M}{1 + \theta\ dt\ \lambda_M} \right| \leq 1, \tag{15}$$

where λ_M is an eigenvalue of the matrix $\mathbf{M}$. The eigenvalues of the matrix $\mathbf{M}$ can be calculated by solving the generalized eigenvalue problem $\mathcal{L}\mathbf{\Phi_d}\boldsymbol{s} = \lambda_M\mathbf{A}\boldsymbol{s}$.

For the case of the Crank-Nicholson scheme ($\theta = 0.5$), the inequality (15) is always satisfied if $\lambda_M \geq 0$. This implies the scheme is unconditionally stable if $\lambda_M \geq 0$.

When $\theta = 0$, we obtain the explicit time-stepping formulation. The condition for stability is

$$|1 - dt\ \lambda_M| \leq 1, \tag{16}$$

i.e.,

$$dt \leq \frac{2}{\lambda_M} \quad \text{and} \quad \lambda_M \geq 0. \tag{17}$$

It can be seen from the inequality (15) that the stability of the collocation schemes depends on three factors, i.e., θ, dt and the eigenvalues of the matrix $\mathbf{M}$ or $\mathbf{M_H}$. As the eigenvalues of matrix $\mathbf{M}$ are difficult to be found explicitly, the stability conditions are checked numerically.

4 Numerical Studies

4.1 1D Unsteady Convection-Diffusion Problem

Consider the following one dimensional problem,

$$\frac{\partial u}{\partial t} = \kappa \frac{\partial^2 u}{\partial x^2} + V \frac{\partial u}{\partial x} \quad 0 < x < 1\ ,\ t > 0, \tag{18}$$

with the following Dirichlet boundary conditions and initial condition

$$u(0,t) = ae^{bt} \ , u(1,t) = ae^{bt-c} \ \ t > 0, \ \ and \ \ u(x,0) = ae^{-cx}.$$

In equation (18), κ is the diffusion coefficient, V is a constant representing the velocity and a,b,c are some arbitrary constants. The analytical solution for the above problem is given by

$$u(x,t) = ae^{bt-cx} \quad \text{where} \quad c = \frac{V \pm \sqrt{V^2 + 4\kappa b}}{2\kappa} > 0. \tag{19}$$

4.1.1 Globally Supported RBFs

The Péclet number for the above problem is defined as $P_e = \frac{V}{\kappa}$. Uniformly distributed collocation points ranging from $N_{\min} = 11$ to $N_{\max} = 101$ have been taken in the 1D domain for studying the convergence trends of each RBF. Figure 1(a)-(c) show the convergence trends of each of the globally supported RBF for $a = 1$, $b = 0.1$, $V = 1$, $\kappa = 1$, $dt = 0.001$, $t_f = 1$ and $\theta = 0.5$, when $P_e = 1.0,\ 10$ and 100.

From Figure 1(a), we find the RBFs incorporating a shape parameter (MQ, IMQ and Gaussian), when properly tuned, have very high convergence rates as compared to higher order TPS or quintics. From this Figure, it can also be seen that the multiquadric (MQ) performs better compared to the other RBFs.

For the case where the convection term slightly outgrows the diffusion term ($P_e = 10$), the analytical solution is not completely smooth and hence for a small number of collocation points, all the RBFs are unable to capture the solution with a high degree of accuracy (see Figure 1(b)). However, MQ, IMQ and Gaussian produce results with errors, $\varepsilon \approx 10^{-3}$. As we increase the number of collocation points, $r^8 \log r$ and $r^6 \log r$ outperform MQ, IMQ and Gaussians.

For the case where the convection term completely dominates over the diffusion term ($P_e = 100$), the analytical solution has a sharp discontinuity near the left boundary. From Figure 1(c), it can be observed that the errors decrease as the number of collocation points increases. The accuracy suffers as compared to the earlier cases of $P_e = 1$ and $P_e = 10$. This can be attributed to the numerical oscillations observed

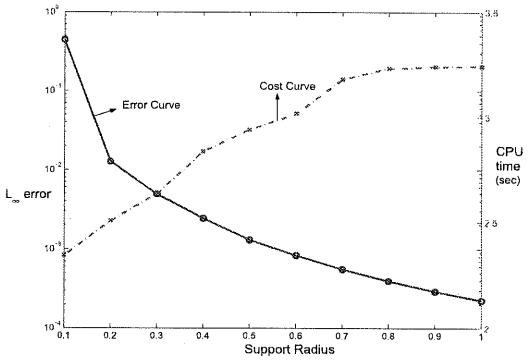

Figure 2. Error norm VS Computational Cost for a compact RBF

in the numerical solution. However, for 271 collocation points spaced regularly in the 1D domain, we obtain errors ε of magnitude $6.600E-03$ ($r^4 \log r$) and $5.068E-04$ (MQ) RBFs. This suggests that in principle, the meshless scheme is capable of capturing the solution given sufficient number of collocation points. The main hinderance being that for a large number of collocation points, the matrix $\mathbf{H}_+$ turns out to be highly ill-conditioned.

Remark: Solving equation (18) using random points collocation (obtained by Sobol sequence), similar results as in the uniformly distributed points were obtained.

4.1.2 Compactly Supported RBFs

Table 2 presents the results obtained when the 1-D convection-diffusion equation was solved using a typical compact kernel [10, 11]. From this table, it can be observed that the support parameter plays the same role as the shape parameter in the global RBFs. The value of the support parameter gives an indication of the sparsity of the resultant coefficient matrix. As the support parameter is increased, the sparsity decreases resulting in a better accuracy but at additional computational cost (Table 2).

Table 2: Results for $\phi = (1-r)_+^6(35r^2+18r+3)$ RBF ([10])
Pe=1.0, a=1.0, b=0.1, v=1.0, κ=1.0, N=51

Support Radius	L_∞ error	CPU time (sec)
0.1	0.4413	2.3449
0.2	0.0127	2.5054
0.3	0.0049	2.6349
0.4	0.0024	2.8369
0.5	0.0013	2.9402
0.6	8.30e-04	3.0150
0.7	5.57e-04	3.1793
0.8	3.95e-04	3.2307
0.9	2.92e-04	3.2393
1.0	2.24e-04	3.2417
1.5	8.26e-05	3.3265

The above results are also presented in Figure 2. Similar results were obtained using $\phi = (1-r)_+^4(4+16r+12r^2+3r^3)$, $(1-r)_+^6(6+36r+82r^2+72r^3+30r^4+5r^5)$ compactly supported RBFs [11].

4.2 2D Unsteady Convection-Diffusion Problem

The governing equation is written as

$$\frac{\partial u}{\partial t} = \kappa_x \frac{\partial^2 u}{\partial x^2} + \kappa_y \frac{\partial^2 u}{\partial y^2} + V_x \frac{\partial u}{\partial x} + V_y \frac{\partial u}{\partial y}, \tag{20}$$

and the boundary conditions are

$$u(0,y,t) = ae^{bt}\left(1 + e^{-c_y y}\right), u(1,y,t) = ae^{bt}\left(e^{-c_x} + e^{-c_y y}\right),$$

$$u(x,0,t) = ae^{bt}\left(1 + e^{-c_x x}\right), u(x,1,t) = ae^{bt}\left(e^{-c_x x} + e^{-c_y}\right),$$

with the initial condition

$$u(x,y,0) = a\left(e^{-c_x x} + e^{-c_y y}\right).$$

The analytical solution is given by

$$u(x,y,t) = ae^{bt}\left(e^{-c_x x} + e^{-c_y y}\right), \tag{21}$$

where

$$c_x = \frac{V_x \pm \sqrt{V_x^2 + 4b\kappa_x}}{2\kappa_x} > 0 \quad \text{and} \quad c_y = \frac{V_y \pm \sqrt{V_y^2 + 4b\kappa_y}}{2\kappa_y} > 0.$$

If we put $V_x = V_y = V$ and $\kappa_x = \kappa_y = \kappa$, for the two dimensional case we can define an analogous Péclet number as $P_e = \frac{V}{\kappa}$. As before, we present the results for the 2D problem for three different Péclet numbers. Uniformly distributed collocation points ranging from $N_{\min} = 6 \times 6$ to $N_{\max} = 25 \times 25$ have been taken in the 2D domain to obtain the convergence trends of each RBF. The values of a, b, V, κ, dt, t_f and θ are taken to be the same as in 1D problem.

Figure 1(d) shows the convergence trends of the RBFs for the 2D problem when $P_e = 1$. As before, σ-tunable RBFs have high convergence rates and accurate results are obtained with TPS provided there are sufficient number of collocation points.

From Figure 1(e) ($P_e = 10$), it can be seen that for a small number of collocation points the errors in the approximation provided by various RBFs are quite high. As we move to the right side of the graph we can get acceptable results for $r^8 \log r$, $r^6 \log r$, MQ and IMQ RBFs.

Figure 1(f) shows the accuracy of various RBFs for $P_e = 100$. All the RBFs with the given set of collocation points are not able to capture the sharp discontinuity present in the analytical solution. This may be attributed to the fact that more number of collocation points are needed to capture the discontinuity.

5 Conclusion

In this paper, meshless schemes were presented for the unsteady convection-diffusion equation. A θ-weighting scheme was used for time stepping. Stability analysis of the meshless schemes was presented for the explicit/implicit time stepping. The convergence trends of seven different globally supported RBFs were examined for Péclet numbers of the order 1, 10 and 100. Numerical results show that these global RBF based meshless schemes achieve good accuracies even for moderate Péclet numbers. From

the numerical results obtained with different RBFs, it can be observed that infinitely differentiable RBFs incorporating a shape parameter (MQ,IMQ and Guassian) produce good results over a variety of mesh spacings. However, global RBFs such as TPS or quintics give accurate results when there is a dense set of collocation points. Moreover, there is no need of σ-tuning in these RBFs. For the high Péclet number problem, it is found the meshless schemes are capable of producing acceptable results provided we increase the number of collocation points. For the compact supported RBFs, it is found that as the support parameter is increased, the sparsity decreases resulting in a better accuracy but at additional computational cost.

References

[1] I. Lubashevsky and V. Gafiychuk, Mathematical description of heat transfer in living tissue, *http://www.arxiv.org/adap-org/9911001* , 2004.

[2] J. R. Sibert, J. Hampton, David A. Fournier, and Peter J. Bills, An advection-diffusion-reaction model for the estimation of fish movement parameters for tagging data, with application to skipjack tuna, *Can. J. Fish Aquat. Sci 56*, 925-938, 1999.

[3] H. G. Roos and M. Stynes and L. Tobiska, Numerical Methods for singularly perturbed differential equations (Convection-Diffusion and Flow Problems), Springer Verlag, 1996, Berlin.

[4] K. W. Morton, numerical solution of convection-diffusion equation, Chapman and Hall, 1995.

[5] O. C. Zienkiewicz and R. L. Taylor, Finite Element Method (5th edition) volume 3 - Fluid Dynamics, Elsevier, 334-, 2000.

[6] E. J. Kansa, Multiquadrics-A scattered data approximation scheme with applications to computation fluid dynamics-I. Surface approximations and partial derivatives estimates, *Comput. Math. Appl.*, **19(8/9)**, 127-145, 1990.

[7] E. J. Kansa, Multiquadrics-A scattered data approximation scheme with applications to computation fluid dynamics-II. Solution to parabolic, hyperbolic and elliptic partial differential equations, *Comput. Math. Appl.*, **19(8/9)**, 147-161, 1990.

[8] B. Fornberg and G. Wright and E. Larsson, Some observations regarding interpolants in the limit of flat radial basis functions, *Comput. Math. Appl.*, **1**, 37-55, 2004.

[9] E. J. Kansa and Y. C. Hon, Circumventing the ill-conditioning problem with multiquadric radial basis functions, *Comput. Math. Appl.*, **39**, 123-137, 2000.

[10] H. Wendland, Piecewise polynomial, positive definite and compactly supported radial functions of minimal degree, *Adv. Comput. Math.*, **4**, 389-396, 1995.

[11] Z. Wu, Compactly supported positive definite radial functions, *Adv. Comp. Math*, **4**, 283-92, 1995.

[12] M. D. Buhmann, A new class of radial basis functions with compact support, *Math. Comput.*, **70**, No 233, 307-318, 2000.

[13] S. M. Wong and Y. C. Hon and M. A. Golberg, Compactly supported radial basis functions for shallow water equations, *Appl. Math. Comput.*, **127**, 79-101, 2002.

[14] J. Li and C. S. Chen, Some observations on unsymmetric radial basis function collocation methods for convection-diffusion problems, *Internat. J Numer. Methods Engrg.*, **57**, No. 8, 1085-1094, 2003.

[15] P.P. Chinchapatnam, K. Djidjeli, P.B. Nair, Unsymmetric and symmetric meshless schemes for the unsteady convection-diffusion equation, *Comput. Meth. Appl. Mech. Engrg.* (under review).

[16] Y. C. Hon and R. Schaback, On unsymmetric collocation by radial basis functions, *Appl. Math. Comput.*, **119**, 177-186, 2001.

[17] C. A. Micchelli, Interpolation of scattered data: distance matrices and conditionally positive definite functions, *Constr. Approx.*, **2**, 11-22, 1986.